EVALUATION OF PAVEMENT ROUGHNESS THROUGH VEHICLE VIBRATION MONITORING

K. Opara & J. Zieliński
Heller Consult sp. z o. o., Poland
kopara@heller-consult.pl, jzielinski@heller-consult.pl
K. Brzeziński
Faculty of Civil Engineering Warsaw University of Technology, Poland
k.brzezinski@il.pw.edu.pl
K. Kaczmarek-Majer
Systems Research Institute Polish Academy of Sciences, Poland
k.kaczmarek@ibspan.waw.pl
M. Bukowicki
Institute of Fundamental Technological Research Polish Academy of Sciences, Poland
mbuk@ippt.pan.pl

ABSTRACT

Driving on uneven roads causes vibrations of the vehicle. Modern smartphones are equipped with accelerometers and gyroscopes which allow for inexpensive acquisition of information about the shaking level. This study reports on field tests of a system, which measures vibrations of a driving vehicle using four smartphones as sensors. The collected data undergo a series of processing steps, namely synchronization, virtual reorientation, temporal and spectral filtering, and assignment of road localization. We use quarter-car and half-car suspension models to retrieve the longitudinal road profile and to compute unevenness indicators. The accuracy of the system was computed by comparison with traditional laser profilometer on an 18.6 km long test section using eight rides with different speeds. It averages to 71% and exceeds 80% for the best calibrated cases. Additionally, we report on the feedback obtained during tests of the system in a district road administration in Poland.

1. INTRODUCTION

Effective decision-making on the maintenance strategies of road network requires information on the road pavement condition. State-of-the-art inspection vehicles simultaneously collect data on the pavement evenness, ruts, surface distresses (cracks, patches), and make panoramic images. Measurements of skid resistance and road deflections are usually done by separate, dedicated vehicles. However, wide scope and high quality of the road condition data comes at a price prohibitively high for local road administrators. Consequently, there is a need for a more affordable solution for objective network-wide surveying.

Proliferation of smartphones creates a possibility to easily measure vibrations during a ride. After clearing the acceleration signal from the influence of the vehicle's suspension and taking into account the driving conditions, most notably speed, it is possible to evaluate the pavement evenness and identify certain surface distresses. In this paper, we report on the field tests of system ASPEN (Accelerometer System for Pavement Evaluation), which allows for approximate road condition assessment with smartphones mounted in a driving car.

2. RELATED STUDIES

The concept of using smartphones to evaluate road roughness is increasingly popular as they combine satellite navigation system and inertial sensors in a compact and commonly available device. Vibration-based measurements performed by smartphones offer significantly lower costs in comparison to laser profiling, at the same time being more reproducible and less labour intensive than visual inspection (Radopoulou et al. 2016, Wahlström et al. 2016, Alavi & Buttlar 2019).

Various aspects are relevant to the evaluation of road quality. In general, two main approaches can be distinguished. First of them concentrates on the identification of point distresses, which cause significant inconvenience for the driver and passengers, such as potholes, bumps or sunken manholes. After detection they can be reported to road administrators and repaired. This type of system was tested e.g. in Boston (Brisimi et al. 2016). A range of studies tested various types of classification algorithms in order to detect point anomalies (Brisimi et al. 2016, Mukherjee & Majhi 2016, Xue et al. 2017, Bello-Salau et al. 2018, Celaya-Padilla et al. 2018, Silva et al. 2018). The second type of road quality evaluation is calculating values of given indices for road segments, typically of the length 20-100 meters. This approach is more compatible with methodology used currently in road maintenance in planning and long-term management, in contrast to the ad hoc maintenance of detected local distresses. On-time diagnostics and proper treatment allow to significantly reduce the overall costs of road maintenance (Alavi & Buttlar 2019, Haas and Hudson 1978). The approach presented in this work focuses on the evaluation of quality of road segments, rather than point anomalies detection.

Among different measures used by road administrators in the decision making process, the most common are International Roughness Index IRI (Mucka 2017), road classes assigned by the power spectral density of the profile (ISO 8608), Present Serviceability Index PSI, German Längsebenheitswirkindex LWI (Ueckermann 2002) and Chinese Riding Quality Index RQI (Yang 2006). The most common indicator is IRI and it is the primary goal for identification by smartphone based systems (Douangphachanh & Oneyama 2014, Forslöf & Jones 2015, Grimmer 2015, Yagi 2017). Estimation of other quality measures is also topic of studies, e.g. for PSI (Aleadelat et al. 2018), RQI (Chen et al. 2016) or profile PSD (González et al. 2008), which is also used in ISO classification. In addition, some new quality indices are proposed (Alessandroni et al. 2014, Badurowicz et al. 2016).

One of the approaches to evaluate the road quality is based on the estimation of its longitudinal profile. It was adopted e.g. by Yagi (2017), Ngwangwa et al. (2014) and Xue et al. (2017). Also some theoretical works (with simulated data) addressed this issue (Noack et al. 2018, Zhang et al. 2018). A significant advantage of profile estimation is that it allows to easily calculate virtually any index of interest which is required by road administrator for the proper maintenance management.

In surface roughness evaluation, an important role is played by mechanical models of car suspensions. They are commonly used in modelling of pavement-car interactions (Agostinacchio et al. 2014, Rath et al. 2015, Tomiyama & Kawamura 2016) and also directly involved in calculation of some of the pavement quality indices, such as IRI or LWI. Mechanical models of car suspension are also a valuable tool for vibration-based road quality evaluation. They significantly reduce the number of parameters which have to be tuned for a given vehicle. They are also physics aware and compatible with methodology used in the field of road diagnostic. The most common type of mechanical model is a

quarter car with a single or two degrees of freedom (Agostinacchio et al. 2014, Xue et al. 2017, Yagi 2017). Half car model is more expressive and allow for pitch rotation of the car body (Gao et al. 2007, Mukherjee & Majhi 2016). Half car models may be especially useful if the sensor (measuring smartphone) is not located directly over one of the car axles. In this work we investigate both quarter and half car models. In the literature, sometimes even the full-car model is considered (Ngwangwa et al. 2014, Noack et al. 2018), however it was not applied to the real world data yet, presumably due to the difficulties in its identification.

In different systems aiming to evaluate the road quality or to detect anomalies many preliminary steps of data analysis are common. Reorientation of the measured accelerations to the vehicle reference frame is well established (Wahlström et al. 2016). Another task is the data filtering, typically performed in order to remove high frequency noise (Mukherjee & Majhi 2016, Aly & Youssef 2015, Xue et al. 2017) and low frequency modes, originating from manoeuvres or macroscale road geometry rather than pavement quality (Astarita et al. 2012, Eriksson et al. 2008, Ghadge et al. 2015, Mohamed et al. 2015). For both purposes often moving average (Xue et al. 2017) or Butterworth filters (Ghadge et al. 2015, Mohamed et al. 2015) are used. Mapping of the measurements on road network can be challenging (Aly & Youssef 2015, Delpriori et al. 2015), however in a typical environment it becomes a standard procedure, in our case conducted by software previously developed in our company.

Practical aspects of the measurements, such as smartphone mounting and the influence of velocity, have been reviewed e.g. by (Sattar et al. 2018). Corrections for the vehicle speed are often necessary (Fazeen et al. 2012, Alessandroni et al. 2017). The influence of smartphone model itself is rather negligible. Results described in the literature suggest that in the problem of road quality estimation, apart from the modelling challenges, also a range of practical aspects plays an important role.

3. MECHANICAL MODELS

One of the features provided by the ASPEN system is road profile computation by using acceleration measured with a smartphone. Road profile data allows for obtaining common ride quality indicators. Two mechanical models of car suspension were implemented, quarter car (QC) and half car (HC). They are presented in Fig. 1. In this section we will briefly present the methodology. Moreover, transfer function for profile computation with HC model are derived.

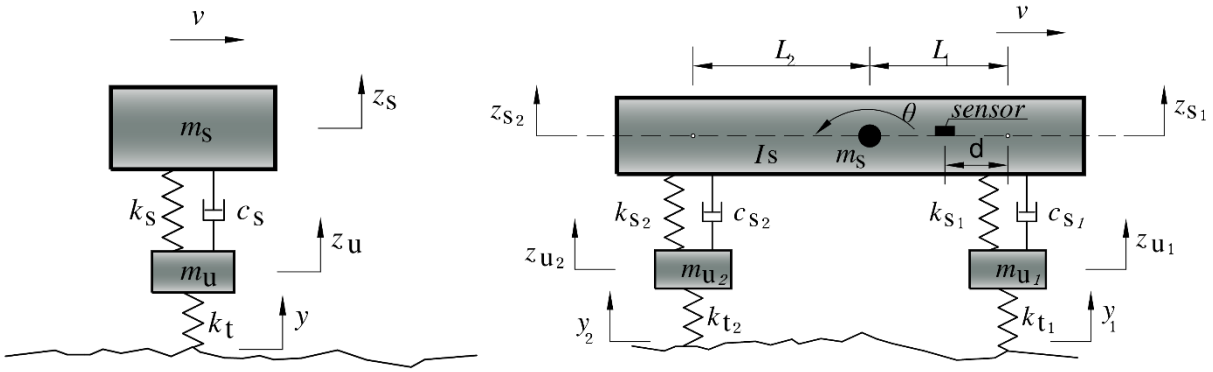

Fig. 1. Schemes of a quarter car and half car models

The QC model consists of five elements:

- k_t – spring coefficient representing the tire,

- m_{u} – unsprung mass representing a half of the axle,
- k_{s} – spring coefficient representing resilient reaction of the vehicle suspension,
- c_{s} – damping coefficient representing the viscous reaction of the vehicle suspension,
- m_{s} – sprung mass representing a quarter of the mass of the vehicle body.

The vibrations of the model elements are excited during the ride over the road profile with speed v. The height of the profile right under the tire is denoted by y. The unsprung and sprung masses of the QC model may experience vertical displacements z_{u} and z_{s} respectively.

The notation for HC model differs only slightly. Since the HC model includes both front and rear suspension elements, they are designated with index 1 for front axle and 2 for rear axle. Moreover, sprung element joining the axles has an additional (rotational) degree of freedom. Therefore, it may rotate around its centre of mass (m_{s}) located with distance L_1 from front axle. The rotary angle is θ and the mass moment of inertia for the car body is I_{s}. It is assumed that angular and vertical accelerations (z_d) may be acquired with sensor (smartphone) located at distance d from front axle.

The general workflow for the computation of the road profile is the following:
- measuring acceleration and vehicle speed with smartphone,
- preprocessing of the measured acceleration (filtering and reorientation),
- transforming the acceleration into the frequency domain with Discrete Fourier Transformation (DFT),
- applying the frequency dependent transfer function $H(\xi)$, which allows for profile $Y(\xi)$ calculation in the frequency domain according to equation (1),
- transforming the profile signal into the spatial domain with inverse DFT,
- post processing (e.g. filtering in order to remove some artificial trends).

$$Y = H \cdot \ddot{Z}_d \tag{1}$$

Further we will focus on the solution for HC model. The transfer function may be derived from the system of motion equations for the model. The motion of the HC model elements is described by the following second order differential equations system (Gao 2007):

$$\boldsymbol{M}\ddot{\boldsymbol{z}} + \boldsymbol{C}\dot{\boldsymbol{z}} + \boldsymbol{K}\boldsymbol{z} = \boldsymbol{p} \tag{2}$$

where:

$$\boldsymbol{M} = \begin{bmatrix} L_2 m_{\mathrm{s}}/(L_1+L_2) & 0 & L_1 m_{\mathrm{s}}/(L_1+L_2) & 0 \\ I_{\mathrm{s}}/(L_1+L_2) & 0 & -I_{\mathrm{s}}/(L_1+L_2) & 0 \\ 0 & m_{\mathrm{u}_1} & 0 & 0 \\ 0 & 0 & 0 & m_{\mathrm{u}_2} \end{bmatrix}, \boldsymbol{C} = \begin{bmatrix} c_{\mathrm{s}_1} & -c_{\mathrm{s}_1} & c_{\mathrm{s}_2} & -c_{\mathrm{s}_2} \\ L_1 c_{\mathrm{s}_1} & -L_1 c_{\mathrm{s}_1} & -L_2 c_{\mathrm{s}_2} & L_2 c_{\mathrm{s}_2} \\ -c_{\mathrm{s}_1} & c_{\mathrm{s}_1} & 0 & 0 \\ 0 & 0 & -c_{\mathrm{s}_2} & c_{\mathrm{s}_2} \end{bmatrix}$$

$$\boldsymbol{K} = \begin{bmatrix} k_{\mathrm{s}_1} & -k_{\mathrm{s}_1} & k_{\mathrm{s}_2} & -k_{\mathrm{s}_2} \\ L_1 k_{\mathrm{s}_1} & -L_1 k_{\mathrm{s}_1} & -L_2 k_{\mathrm{s}_2} & L_2 k_{\mathrm{s}_2} \\ -k_{\mathrm{s}_1} & k_{\mathrm{s}_1} + k_{\mathrm{t}_1} & 0 & 0 \\ 0 & 0 & -k_{\mathrm{s}_2} & k_{\mathrm{s}_2} + k_{\mathrm{t}_2} \end{bmatrix}, \boldsymbol{z} = \begin{bmatrix} z_{\mathrm{s}1} \\ z_{\mathrm{u}1} \\ z_{\mathrm{s}2} \\ z_{\mathrm{u}2} \end{bmatrix}, \boldsymbol{p} = \begin{bmatrix} 0 \\ 0 \\ k_{\mathrm{t}_1} y_1 \\ k_{\mathrm{t}_2} y_2 \end{bmatrix}$$

After application of Fourier transformation we obtain an equation in the frequency domain:

$$\boldsymbol{M}\ddot{\boldsymbol{Z}} + \boldsymbol{C}\dot{\boldsymbol{Z}} + \boldsymbol{K}\boldsymbol{Z} = \boldsymbol{P} \tag{3}$$

The properties of Fourier transformation imply relations:

$$\dot{Z}_{\mathrm{i}} = \frac{1}{2\pi j\xi}\ddot{Z}_{\mathrm{i}} \tag{4}$$

$$Z_{\mathrm{i}} = \frac{-1}{4\pi^2\xi^2}\ddot{Z}_{\mathrm{i}} \tag{5}$$

therefore:

$$\left(\boldsymbol{M} + \frac{1}{2\pi j\xi}\boldsymbol{C} + \frac{-1}{4\pi^2\xi^2}\boldsymbol{K}\right)\ddot{\boldsymbol{Z}} = \boldsymbol{P} \tag{6}$$

where j is the imaginary unit. Relation between y_1 and y_2 in the time domain is as follows:

$$y_2(t + \Delta t) = y_1(t) \tag{7}$$

where $\Delta t = \frac{L_1 + L_2}{v}$. It can be expressed in frequency domain by equation:

$$Y_2 = Y_1 e^{-2\pi j\Delta t} \tag{8}$$

Thus, vector $\boldsymbol{P}$ may be rewritten as:

$$\boldsymbol{P} = \begin{bmatrix} 0 \\ 0 \\ k_{\mathrm{t}_1} Y_1 \\ k_{\mathrm{t}_2} Y_1 e^{-2\pi j\Delta t} \end{bmatrix}$$

Hence, we have five unknown values and four equations. After measurement of the acceleration in single point of the vehicle we will be able to compute the road profile.

Let us introduce matrix $\boldsymbol{A}$,

$$\boldsymbol{A} = \left(\boldsymbol{M} + \frac{1}{2\pi j\xi}\boldsymbol{C} + \frac{-1}{4\pi^2\xi^2}\boldsymbol{K}\right) \tag{9}$$

so the equation (6) may be rewritten as:

$$\boldsymbol{A}\ddot{\boldsymbol{Z}} = \boldsymbol{P} \tag{10}$$

In order to express Y_1 using only $\ddot{Z}_1$ we need to calculate vector $\boldsymbol{N}$:

$$\boldsymbol{N} = \boldsymbol{B}^{-1}\boldsymbol{R} \tag{11}$$

where

$$\boldsymbol{B} = \begin{bmatrix} A_{12} & A_{13} & A_{14} \\ A_{22} & A_{23} & A_{24} \\ A_{42} - A_{32}s & A_{43} - A_{33}s & A_{44} - A_{34}s \end{bmatrix},\ \boldsymbol{R} = \begin{bmatrix} -A_{11} \\ -A_{21} \\ A_{31}s - A_{41} \end{bmatrix},\ s = \frac{k_{\mathrm{t}_2} e^{-2\pi j\Delta t}}{k_{\mathrm{t}_1}}$$

Therefore:

$$P_1 = \ddot{Z}_1(A_{31} + A_{32}N_1 + A_{33}N_2 + A_{34}N_3) = \ddot{Z}_1 H' \tag{12}$$

Transfer function H' allows for calculation of P_1 when $\ddot{Z}_1$ is known. Nonetheless, acceleration measured by sensor ($\ddot{Z}_d$) is a combination of $\ddot{Z}_1$ and $\ddot{Z}_2$:

$$\ddot{Z}_d = \frac{\ddot{Z}_1 - \ddot{Z}_2}{L_1 + L_2}(L_1 + L_2 - d) + \ddot{Z}_2 \tag{13}$$

thus,

$$\ddot{Z}_1 = \frac{\ddot{Z}_d(L_1 + L_2)}{L_1 + L_2 - d(1 + N_2)} \tag{14}$$

Finally, Y_1 may be calculated as:

$$Y_1 = \ddot{Z}_d \frac{(L_1 + L_2)H'}{k_{t_1}[L_1 + L_2 - d(1 + N_2)]} = \ddot{Z}_d H \tag{15}$$

where the transfer function is denoted as H.

4. RESULTS

The ASPEN system was verified in a field experiment conducted in Warsaw, Poland on a 18.6 km long test section repeated eight times in the Ford Transit van, Fig. 2. As a source of reference data we used measurements done earlier in 2018 using a survey vehicle equipped with laser profilometer by the Road and Bridge Research Institute (IBDiM).

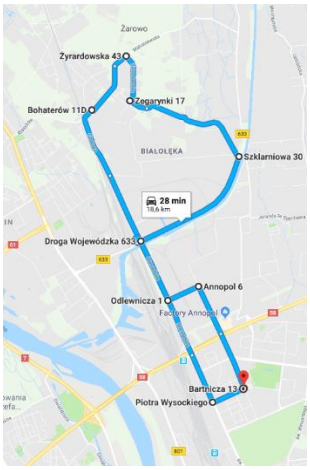

Fig. 2. Field test route; map source Google Maps

4.1. Reference acceleration

Based on the reference measurements of the road profile, we calculated the accelerations, which are expected to be experienced by the car body. For this purpose we used quarter and half car models and numerical integration of the relevant system of ordinary differential equations. In the QC model, we used the “golden car” parameters (Sayers & Karamihas 1998), while for the HC model, two variants of the parameters are considered: (a) the parameters reported by Gao et al. (2007); (b) optimal parameters found within the calibration procedure performed for the considered vehicle type (Ford Transit commercial van). For the purpose of calibration, we performed multiple passages with various speed over several speed bumps with known shape and height. Optimal

parameters were obtained by minimisation of the difference between the acceleration measured with smartphones and the one calculated with half car model. In the minimisation, we took into account some known physical constraints, such as the total length of the car or the ratio of sprung and unsprung masses. Having collected and processed the reference profile and accelerations, the results were compared with the accelerations measured with four smartphones using the ASPEN app.

4.2. Measurement setup

During each ride, recordings from four smartphones (ASUS ZenFone 3 Z017D) were gathered and processed. Each smartphone measured vertical acceleration at a constant 250 Hz frequency. This corresponds to spatial resolution of the order of 7 cm at velocity 60 km/h and 3 cm at 30 km/h. The position and speed of the vehicle was updated every second by the satellite navigation module. Higher spatial resolution was obtained by interpolation of these values, as they are relatively smooth. Therefore, in terms of space resolution, smartphone measurements offer sufficient accuracy.

Since the sensitivity of all sensors were slightly different, even though the smartphones were of the same type, the vertical acceleration signal was normalized so that the mean value during the experiment equals 9.81 m/s. Fig. 3. presents mounting of the four smartphones included in this field experiment.

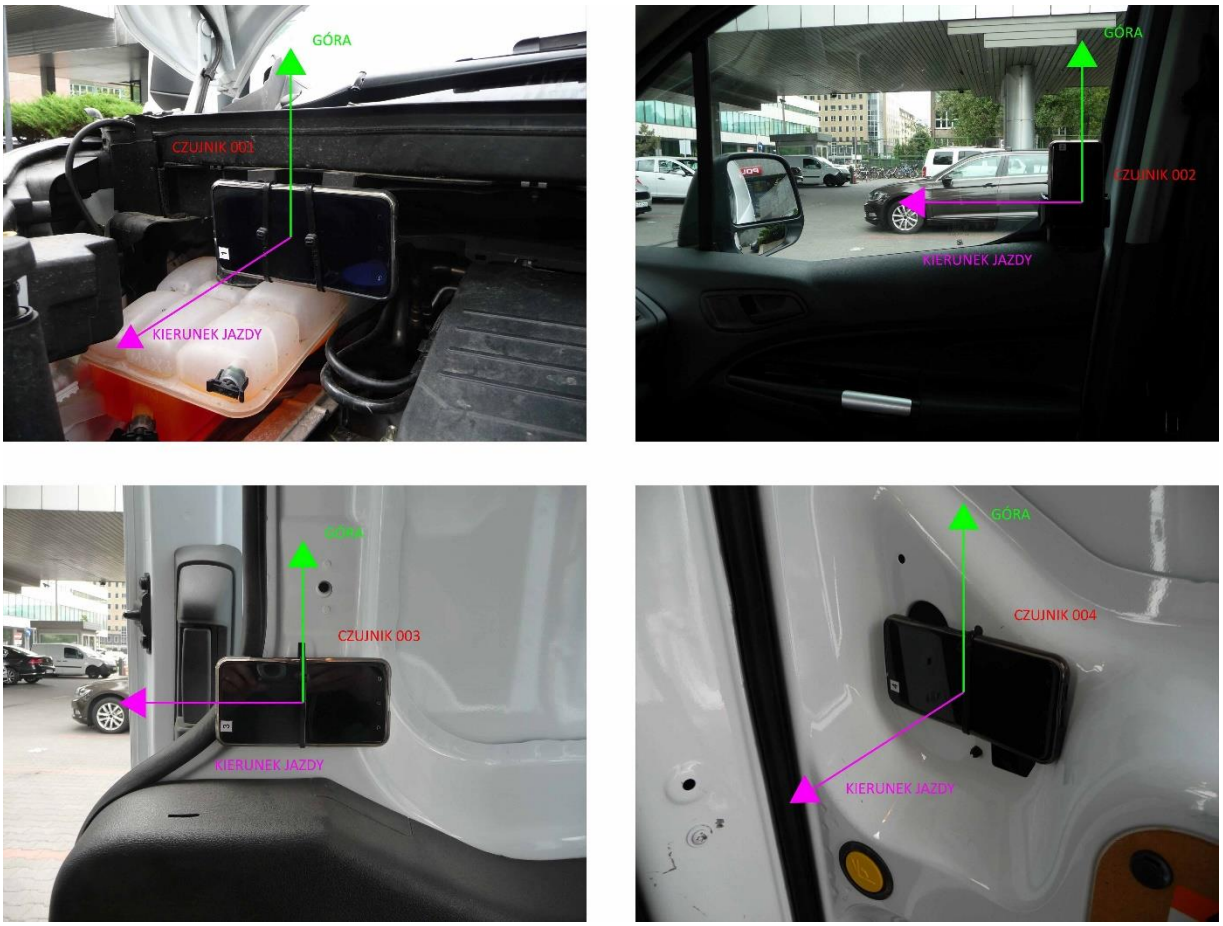

Fig. 3. Mounting of the four smartphones in this experiment; green arrow indicated direction up and magenta arrow indicates the driving direction.

The first smartphone was located under the bonnet, the second on a side window, the third on a side of the cargo area and the fourth on the rear, cargo doors. The first, third and fourth smartphone were fixed with cable ties while the second was mounted on a handle attached to a window.

4.3. Comparison of measured and reference accelerations

The primary purpose of the conducted statistical analysis was to compare the accelerations measured by smartphones of the ASPEN application and the reference accelerations retrieved with the QC model (golden car) and the HC models. Fig. 4. presents an example of of the reference acceleration (based on the QC model) and the acceleration measured by smartphone from one ride of this field experiment.

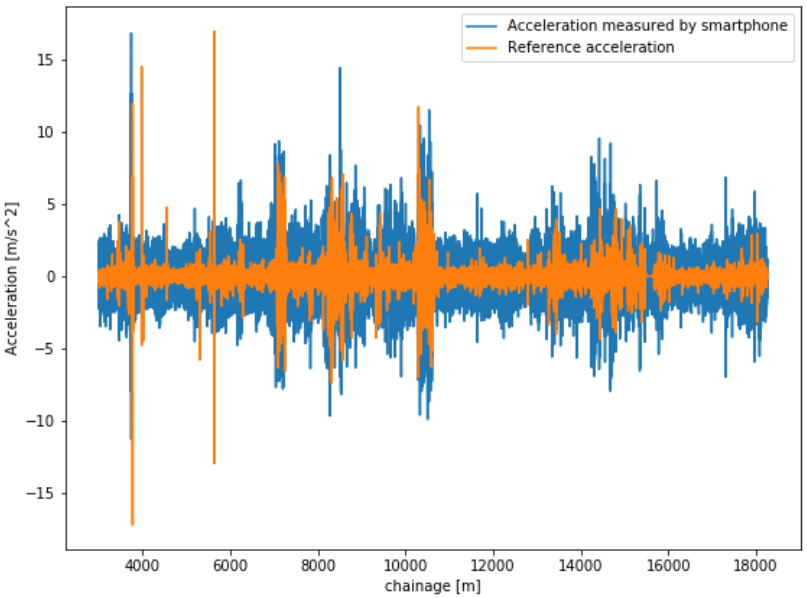

Fig. 4. Reference accelerations (from QC model) and accelerations measured by one smartphone.

Distance in meters (chainage) was calculated based on projection of satellite navigation readings, which was locally enhanced with “smartphone odometer” readings obtained from smartphones’ data on speed and timestamps. Next, the standard deviation (SD) of the accelerations of the sequential, overlapping segments of 50 meters are calculated and further processed. Fig. 5. illustrates the dependence between the vehicle speed and the standard deviation (SD) of the reference acceleration (based on the QC model) of the 50 m segments and the SD of the acceleration measured by smartphone.

Shades of green in Fig. 5 illustrate the speed of the vehicle during smartphone-based measurements. There exists correlation between the reference and measured data. However, as illustrated in Fig. 4, the variability of the reference acceleration is constantly lower than the variability of the accelerations measured with smartphone. To verify this observation, the 0.25, 0.5 and 0.75 quantiles of the preprocessed series were calculated and compared with the Manhattan distance for all measurements of this experiment. Table 1. presents the resulting quantiles.

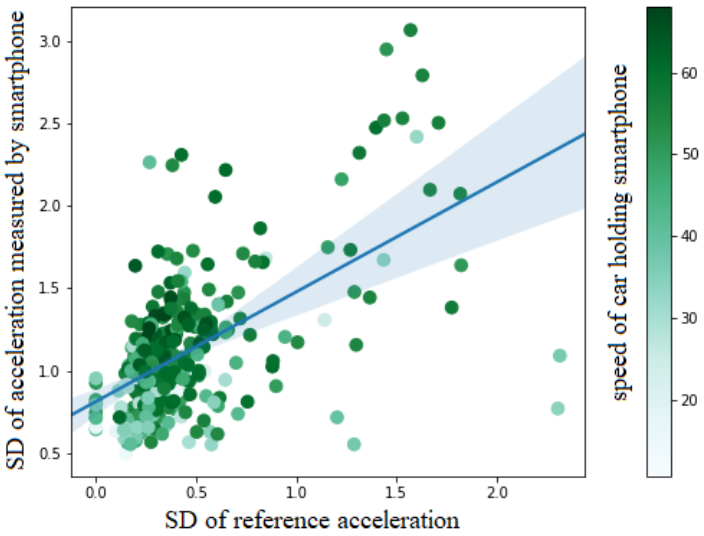

Fig. 5. Dependence between the vehicle speed and the standard deviation (SD) of the reference acceleration

Table. 1. Mean and SD of 0.25/0.5/0.75 quantiles comparison for the reference accelerations (R) and measured accelerations (M) according to the Golden Car model.

	0.25 quantile	**0.5 quantile**	**0.75 quantile**
Difference (R - M)	-0.39 ± 0.13	-0.46 ± 0.16	−0.60 ± 0.16

As presented in Table 1, all three considered quantiles confirm that the standard deviation of the reference accelerations is lower. Therefore, we introduce the calibration period at the beginning of each ride to shift the measured by a constant term. First 3 km of the route were used to calibrate the model and the remaining 15.6 km are used to evaluate the similarity between time series holding standard deviation of measured and reference accelerations for the sliding segments of 50 m. In Fig. 6, the standard deviation (SD) of the reference and measured accelerations from the exemplary ride before and after the calibration are presented.

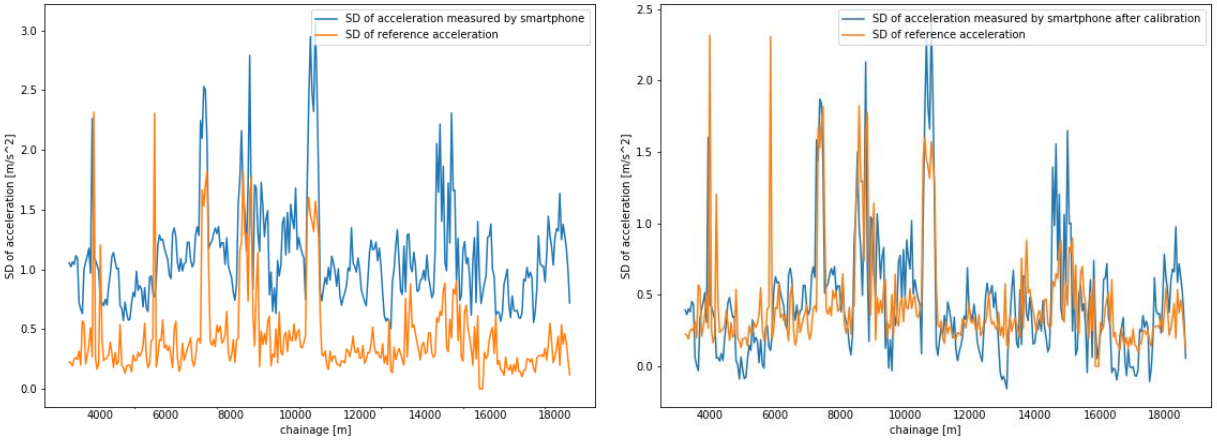

Fig. 6. Standard deviation (SD) of the reference and smartphone accelerations for sliding segments of 50 m (a) before calibration and (b) after calibration.

Recent experimental comparison of nine different similarity measures and their variants for time series by Wang et al. (2013) suggest that for large data classical lock-step measures (e.g., Manhattan distance) yield similar results to the elastic measures (e.g., dynamic time warping DTW). Consequently, in our study, the similarity between two time series, *a* and *b,* was calculated using the relative Manhattan similarity degree defined as

$$s_{a,b} = 1 - \sum_{i=1}^{n} \frac{|a_i - b_i|}{|a_i| + |b_i|} \quad (16)$$

where time series *a* and *b* have length *n*.

In Table 2 and Fig. 7 the average degrees of similarity for series with measured and reference accelerations are presented. We distinguish the resulting similarity for the considered four sensors and two considered mechanical models and their variants.

Table 2. Mean and standard deviation of similarity degree for SD of reference accelerations (HC and QC models) and SD of accelerations measured by smartphones for sliding segments of 50 m

Data source	**QC ("golden car")**	**HC Gao et al (2007)**	**HC (Calib. for Ford 1)**	**HC (Calib. for Ford 2)**
Smartphone 1	66.3% ± 2.2%	55.4% ± 3.0%	61.7% ± 2.2%	64.5% ± 2.0%
Smartphone 2	62.0% ± 6.7%	44.9% ± 5.1%	52.0% ± 5.3%	56.1% ± 5.9%
Smartphone 3	72.7% ± 4.4%	52.7% ± 5.4%	76.4% ± 2.0%	**81.4% ± 1.3%**
Smartphone 4	56.9% ± 6.6%	40.5% ± 4.3%	**81.3% ± 0.5%**	**81.2% ± 1.2%**
mean	64.4% ± 8.0%	47.9% ± 7.4%	68.3% ± 12.5%	**71.3% ± 11.8%**

The mean similarity degree is the highest for the HC model calibrated based on the vehicle type that was used to hold the ASPEN application. For this model, the mean similarity amounts on average 71%. Moreover, we observe high repeatability of individual sensors, which shows that good measurement setup coupled with appropriate calibration can lead to accuracies consistently exceeding 80%. However, when the parameters in the HC are chosen inadequately, the similarity is also dissatisfactory and amounts to less than 50%. Therefore, it is essential to ensure proper measurement conditions and perform calibration to find optimal parameters. In addition, the use of several smartphones at once gives the potential to increase accuracy.

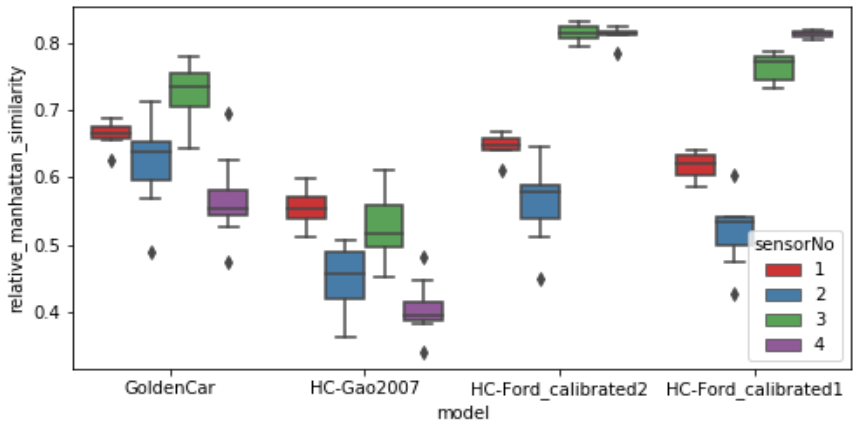

Fig. 7. Boxplots for the similarity degree for reference accelerations (Half Car vs QC models) and accelerations measured by smartphones calculated for sequential segments of 50 meters.

5. USER ENGAGEMENT

5.1. Feedback on system requirements

To identify users' needs and requirements towards the ASPEN system, a survey was carried out among students of civil engineering at the Rzeszów University of Technology as a part of the "Road information systems" course. We collected 12 surveys indicating i.a. strong interest in smartphone-based monitoring of the pavement condition but also a clear expectation that the accuracy and reliability of this new technology is evaluated, Fig. 8.

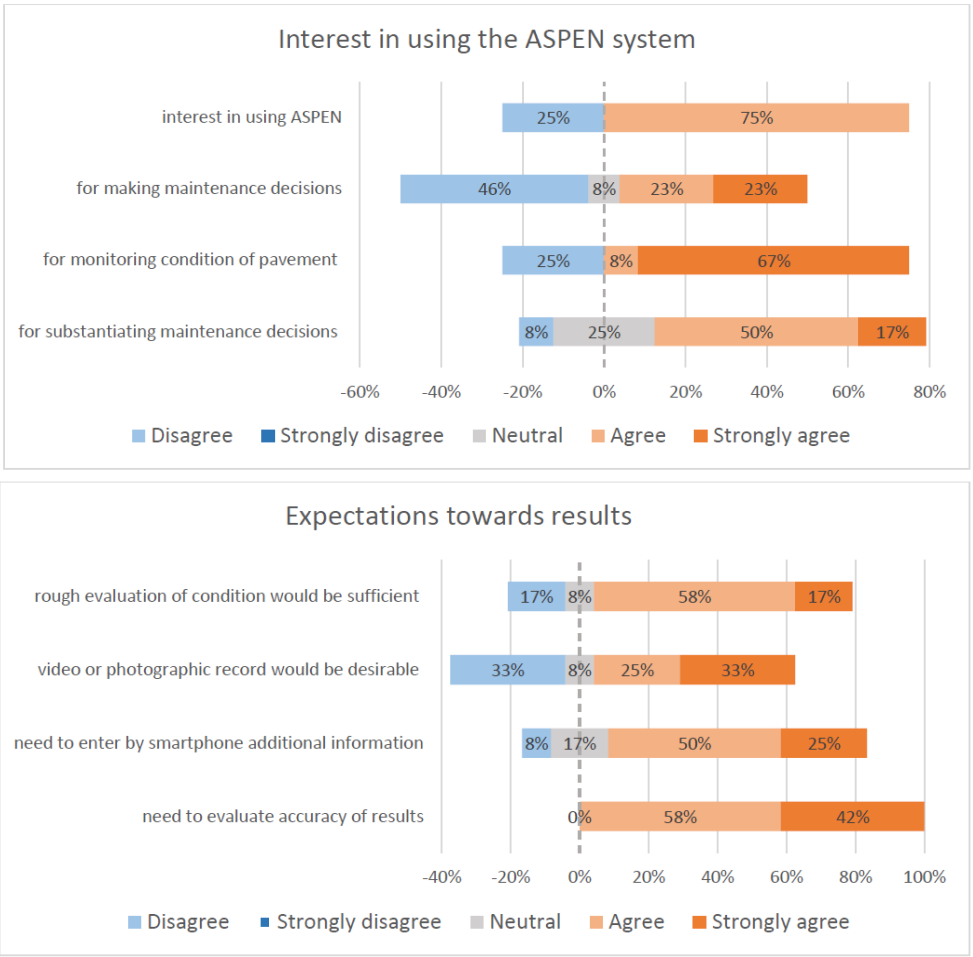

Fig. 8. Some results from the user surveys.

The survey served as a basis for in-depth interviews with several representatives of district level road administrations. The most important feedback collected concerned necessity to integrate the application with routine inspection of roads and adding a functionality of taking photographs, e.g. concerning safety issues or related to the inspection. The results should be provided on-line in the form of maps, graphs (profiles) and documents.

5.2. Application test by District Road Authority in Lidzbark Warmiński, Poland

To pursue user-centric development of the ASPEN system it was send to the Director of District Road Authority (ZDP) in Lidzbark Warmiński – the operator of a low-level road network. He acted as an "alpha customer", an early adopter of the technology providing feedback on its usage and results.

Fig. 9. Five smartphones of the ASPEN system together with supplementary equipment.

Five smartphones with the ASPEN application installed were delivered as well as all the supplemental equipment (handles, chargers, manual, quick start guide), Fig. 9.

The customer drove a few times over his whole network. His overall perception of the system and results was positive, however, he proposed some improvements to the user interface of the smartphone application and suggested a choice of handles, which grip the window stronger. Moreover, he indicated interest in measurements on unpaved roads.

Fig. 10 presents the results of the user measurements. They are presented separately for each driving direction. The elementary data was attributed spatial location with resolution of 1 m and is shown as small, black histograms. For convenient presentation, these data were aggregated into diagnostic sections of 50 m. Their colours show the assessment of road condition based on vertical accelerations (the inner band) and on pitch (the outer band). Pitch was obtained from gyroscope after virtual device reorientation. It is an additional data source related to the pavement evenness, which can support identification of the half-car model.

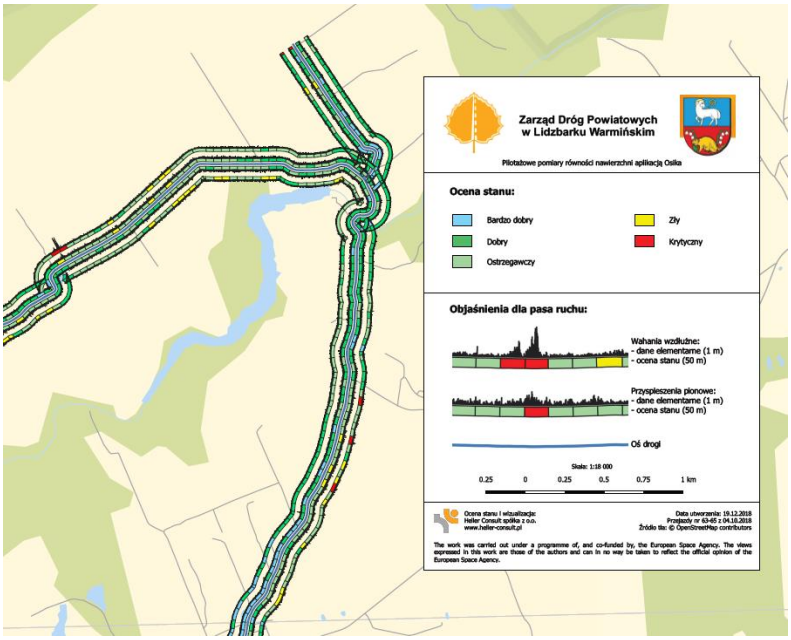

Fig. 10. A map presenting the pavement condition evaluation; background source: OpenStreetMap.

6. CONCLUSIONS

This paper reports on operation principles and field tests of ASPEN system, which performs road evenness diagnostics using smartphones mounted in a driving vehicle. The system is based on mechanical quarter car and half car models. The latter is more general, as it allows for pitch rotation of the vehicle, yet more difficult to correctly identify in a calibration process.

The system was tested on an 18.6 km loop. The measured, vertical accelerations were compared against the accelerations expected to be experienced by the vehicle body. The latter were computed using the road profile obtained with standard, laser profilometer. Results indicate high repeatability of the system and accuracy ranging from 64% to 71% and exceeding 80% for the best calibrated smartphones.

The ASPEN system was also used by the road operator of a district road network in north-eastern Poland, yielding positive feedback about its operation and results.

The obtained results are satisfactory and sufficient for supporting local road administrations with objective network-wide survey data. Nevertheless, there is still significant room for improvement concerning particular processing steps, the model identification and calibration to different vehicle types. These tasks can be supported by hybridizing mechanical models with machine learning methods. Finally, there are some more practical needs such as ensuring high reliability and ease of use, integration with other functionalities, such as taking photographs and making notes, and streamlining of the whole procedure.

ACKNOWLEDGMENTS

The authors are grateful to Dariusz Iskra, the Director of ZDP Lidzbark Warmiński for his engagement in the tests of the ASPEN system. We would also like to thank the employees of Heller Consult sp. z o. o. for their work in preparing, conducting, and processing measurements, in particular Andrzej Nadowski, Marta Mączko, Piotr Pasiński, Arkadiusz Dyczkowki, and Paulina Grudzińska.

The work was carried out under a programme of, and cofunded by, the European Space Agency. The views expressed in this work are those of the authors and can in no way be taken to reflect the official opinion of the European Space Agency.

REFERENCES

1. Agostinacchio, M., Ciampa, D., & Olita, S. (2014). The vibrations induced by surface irregularities in road pavements–a Matlab® approach. *European Transport Research Review*, *6*(3), 267.
2. Alavi, A. H., & Buttlar, W. G. (2019). An overview of smartphone technology for citizen-centered, real-time and scalable civil infrastructure monitoring. *Future Generation Computer Systems*, *93*, 651-672.
3. Aleadelat, W., Wright, C. H., & Ksaibati, K. (2018). Estimation of Gravel Roads Ride Quality Through an Android-Based Smartphone. *Transportation Research Record*, 0361198118758693.
4. Alessandroni, G., Klopfenstein, L. C., Delpriori, S., Dromedari, M., Luchetti, G., Paolini, B., ... & Bogliolo, A. (2014). Smartroadsense: Collaborative road surface condition monitoring. *Proc. of UBICOMM-2014. IARIA*, 210-215.
5. Alessandroni, G., Carini, A., Lattanzi, E., Freschi, V., & Bogliolo, A. (2017). A study on the influence of speed on road roughness sensing: The SmartRoadSense case. *Sensors*, *17*(2), 305.

6. Aly, H., & Youssef, M. (2015, November). semMatch: Road semantics-based accurate map matching for challenging positioning data. In *Proceedings of the 23rd SIGSPATIAL International Conference on Advances in Geographic Information Systems* (p. 5). ACM.
7. Astarita, V., Caruso, M. V., Danieli, G., Festa, D. C., Giofrè, V. P., Iuele, T., & Vaiana, R. (2012). A mobile application for road surface quality control: UNIquALroad. *Procedia-Social and Behavioral Sciences*, *54*, 1135-1144.
8. Badurowicz, M., Cieplak, T., & Montusiewicz, J. (2016, June). The cloud computing stream analysis system for road artefacts detection. In *International Conference on Computer Networks* (pp. 360-369). Springer, Cham.
9. Bello-Salau, H., Aibinu, A. M., Onumanyi, A. J., Onwuka, E. N., Dukiya, J. J., & Ohize, H. (2018). New road anomaly detection and characterization algorithm for autonomous vehicles. *Applied Computing and Informatics*.
10. Brisimi, T. S., Cassandras, C. G., Osgood, C., Paschalidis, I. C., & Zhang, Y. (2016). Sensing and classifying roadway obstacles in smart cities: The street bump system. *IEEE Access*, *4*, 1301-1312.
11. Celaya-Padilla, J., Galván-Tejada, C., López-Monteagudo, F., Alonso-González, O., Moreno-Báez, A., Martínez-Torteya, A., ... & Gamboa-Rosales, H. (2018). Speed bump detection using accelerometric features: a genetic algorithm approach. *Sensors*, *18*(2), 443.
12. Chen, K., Tan, G., Lu, M., & Wu, J. (2016). CRSM: a practical crowdsourcing-based road surface monitoring system. *Wireless Networks*, *22*(3), 765-779.
13. Delpriori, S., Freschi, V., Lattanzi, E., & Bogliolo, A. (2015). Efficient algorithms for accuracy improvement in mobile crowdsensing vehicular applications. *UBICOMM 2015*, 158.
14. Douangphachanh, V., & Oneyama, H. (2014). Exploring the use of smartphone accelerometer and gyroscope to study on the estimation of road surface roughness condition. In *2014 11th International Conference on Informatics in Control, Automation and Robotics (ICINCO)* (Vol. 1, pp. 783-787). IEEE.
15. Eriksson, J., Girod, L., Hull, B., Newton, R., Madden, S., & Balakrishnan, H. (2008, June). The pothole patrol: using a mobile sensor network for road surface monitoring. In *Proceedings of the 6th international conference on Mobile systems, applications, and services* (pp. 29-39). ACM.
16. Fazeen, M., Gozick, B., Dantu, R., Bhukhiya, M., & González, M. C. (2012). Safe driving using mobile phones. *IEEE Transactions on Intelligent Transportation Systems*, *13*(3), 1462-1468.
17. Forslöf, L., & Jones, H. (2015). Roadroid: Continuous road condition monitoring with smart phones. *Journal of Civil Engineering and Architecture*, *9*(4), 485-496.
18. Gao, W., Zhang, N., & Du, H. P. (2007). A half-car model for dynamic analysis of vehicles with random parameters. In 5th Australasian Congress on Applied Mechanics (ACAM 2007) (Vol. 1, pp. 595-600). Engineers Australia.
19. Ghadge, M., Pandey, D., & Kalbande, D. (2015). Machine learning approach for predicting bumps on road. In *2015 International Conference on Applied and Theoretical Computing and Communication Technology (iCATccT)* (pp. 481-485). IEEE.
20. González, A., O'Brien, E. J., Li, Y. Y., & Cashell, K. (2008). The use of vehicle acceleration measurements to estimate road roughness. *Vehicle System Dynamics*, *46*(6), 483-499.
21. Grimmer, D. (2015). Speaker phone: new app tells you degree of road roughness. *Roads & Bridges*, *53*(10).
22. Haas, R., & Hudson, W. R. (1978). *Pavement management systems*, McGraw-Hill.
23. Mohamed, A., Fouad, M. M. M., Elhariri, E., El-Bendary, N., Zawbaa, H. M., Tahoun, M., & Hassanien, A. E. (2015). RoadMonitor: An intelligent road surface condition monitoring system. In *Intelligent Systems' 2014* (pp. 377-387). Springer, Cham.
24. Múčka, P. (2017). International Roughness Index specifications around the world. *Road Materials and Pavement Design*, *18*(4), 929-965.
25. Mukherjee, A., & Majhi, S. (2016). Characterisation of road bumps using smartphones. *European Transport Research Review*, *8*(2), 13.
26. Noack, M., Botha, T., Hamersma, H. A., Ivanov, V., Reger, J., & Els, S. (2018, March). Road profile estimation with modulation function based sensor fusion and series expansion for input reconstruction. In *2018 IEEE 15th International Workshop on Advanced Motion Control (AMC)* (pp. 547-552). IEEE.
27. Radopoulou, S. C., Brilakis, I., Doycheva, K., & Koch, C. (2016). A framework for automated pavement condition monitoring. In *Construction Research Congress 2016* (pp. 770-779).
28. Rath, J. J., Veluvolu, K. C., & Defoort, M. (2015). Simultaneous estimation of road profile and tire road friction for automotive vehicle. *IEEE Transactions on Vehicular Technology*, *64*(10), 4461-4471.
29. Sattar, S., Li, S., & Chapman, M. (2018). Road surface monitoring using smartphone sensors: a review. *Sensors*, *18*(11), 3845.

30. Sayers M, Karamihas SM (1998) The Little Book of Profiling. Basic information about measuring and interpreting road profiles. The regent of the University of Michigan. http://www.umtri.umich.edu/content/LittleBook98R.pdf
31. Silva, N., Shah, V., Soares, J., & Rodrigues, H. (2018). Road anomalies detection system evaluation. *Sensors*, *18*(7), 1984.
32. Tomiyama, K., & Kawamura, A. (2016). Application of lifting wavelet transform for pavement surface monitoring by use of a mobile profilometer. *International Journal of Pavement Research and Technology*, *9*(5), 345-353.
33. Ueckermann, A. (2002). *Der Längsebenheitswirkindex LWI* (No. 839). (*in German*)
34. Wahlström, J., Skog, I., & Händel, P. (2017). Smartphone-based vehicle telematics: A ten-year anniversary. *IEEE Transactions on Intelligent Transportation Systems*, *18*(10), 2802-2825.
35. Wang, X., Mueen, A., Ding, H., Trajcevski, G., Scheuermann, P., & Keogh, E. (2013). Experimental comparison of representation methods and distance measures for time series data. *Data Mining and Knowledge Discovery*, *26*(2), 275-309. https://doi.org/10.1007/s10618-012-0250-5
36. Xue, G., Zhu, H., Hu, Z., Yu, J., Zhu, Y., & Luo, Y. (2017). Pothole in the dark: Perceiving pothole profiles with participatory urban vehicles. *IEEE Transactions on Mobile Computing*, *16*(5), 1408-1419.
37. Yagi, K. (2017) Response type roughness measurement and cracking detection method by using smartphone. In: WCPAM (World Conference on Pavement and Asset Management).
38. Yang, S. (2006). Technical code of maintenance for urban road CJJ36-2006.
39. Zhang, Z., Sun, C., Bridgelall, R., & Sun, M. (2018). Road profile reconstruction using connected vehicle responses and wavelet analysis. *Journal of Terramechanics*, *80*, 21-30.